Cellular/Molecular

# Distinct Mechanisms for Neurotrophin-3-Induced Acute and Long-Term Synaptic Potentiation

**Hyun-Soo Je,[1,2]* Jianzheng Zhou,[1]* Feng Yang,[1] and Bai Lu[1]**

[1]Section on Neural Development and Plasticity, National Institute of Child Health and Human Development, and Gene, Cognition, and Psychosis Program, National Institute of Mental Health, National Institutes of Health, Bethesda, Maryland 20892-3714, and [2]Genetics Graduate Program, George Washington University, Washington, DC 20052

**Although neurotrophins elicit both acute and long-term effects, it is unclear whether the two modes of action are mediated by the same or different mechanisms. Using neuromuscular junction (NMJ) as a model system, we identified three characteristic features required for long-term, but not acute, forms of synaptic modulation by neurotrophin-3 (NT-3): endocytosis of NT-3-receptor complex, activation of the PI3 kinase substrate Akt, and new protein synthesis. Long-term effects were eliminated when NT-3 was conjugated to a bead that was too large to be endocytosed or when dominant-negative dynamin was expressed in presynaptic neurons. Presynaptic inhibition of Akt also selectively prevented NT-3-mediated long-term effects. Blockade of protein translation by the mammalian target of rapamycin inhibitor rapamycin prevented the long-term structural and functional changes at the NMJ, without affecting the acute potentiation of synaptic transmission by NT-3. These results reveal fundamental differences between acute and long-term modulation by neurotrophins.**

*Key words:* **synaptogenesis; *Xenopus*; TrkC; internalization; synaptic plasticity; FM dye; synaptic varicosity**

## Introduction

Neurotrophins, a family of structurally and functionally related proteins that include nerve growth factor (NGF), brain derived neurotrophic factor (BDNF), neurotrophin-3 (NT-3), and neurotrophin-4/5(NT-4/5), have recently emerged as major regulatory factors for synapse development and plasticity (McAllister et al., 1999; Poo, 2001; Lu, 2003). Recent studies indicate that synaptic actions of neurotrophins can be divided into two temporally distinct modes: acute effect occurring within seconds or minutes after exposure to a neurotrophin and long-term effects taking hours and days to accomplish (Lu, 2004). In addition, the acute actions of neurotrophins are often associated with the strengthening of preexisting synapses, whereas long-term ones involve formation of new synaptic connections. For example, at cultured *Xenopus* neuromuscular synapses, acute application of a neurotrophin elicits a rapid and transient enhancement of synaptic transmission that requires continuous presence of the factors (Lohof et al., 1993). In contrast, long-term treatment with the same neurotrophin induces a profound change in synaptic efficacy that persists even after withdrawal (Wang et al., 1995). Furthermore, long-term treatment with NT-3 elicits a series of morphological changes that include axonal arborization and synaptic growth (Wang et al., 1995). In hippocampal slices, acute application of BDNF facilitates early phase long-term potentiation (Figurov et al., 1996), but long-term treatment with BDNF increases synapse number and spine density in dendrites of pyramidal neurons, together with modulation of synaptic efficacy (Tyler and Pozzo-Miller, 2001; Ji et al., 2005).

Although the acute and long-term synaptic effects by neurotrophins have been widely observed, little is known about molecular mechanisms underlying these two temporally distinct modes. Initial signaling events by the two modes may be similar. Binding of a neurotrophin to a specific Trk receptor induces its tyrosine kinase activity, leading to the activation of kinase pathways, including phosphatidylinositol 3-kinase (PI3K), mitogen-activated protein (MAP) kinase, and phospholipase C-$\gamma$ (PLC-$\gamma$) (Kaplan and Miller, 2000; Huang and Reichardt, 2003). Unlike other growth factors, internalization of the neurotrophin-Trk receptor complex (endocytosis) triggers signaling events that are quite different from those occurring on the cell surface, thereby mediating unique biological functions of neurotrophins (Riccio et al., 1997; Watson et al., 1999; York et al., 2000; Zhang et al., 2000; Watson et al., 2001).

Studies that examine the molecular mechanisms underlying synaptic actions of neurotrophins have been hampered primarily by difficulties in altering gene expression at presynaptic and postsynaptic sites, particularly for synapses in the CNS. To overcome these difficulties, we used the *Xenopus* neuromuscular synapses, in which specific gene products can be expressed selectively presynaptically or postsynaptically. Here, we demonstrate at least three important factors that distinguish the acute and long-term effects of NT-3: endocytosis of NT-3-receptor complex, activa-

Received May 31, 2005; revised Nov. 2, 2005; accepted Nov. 4, 2005.

We thank Shouson Szu for help and advice on NT-3-beads experiments, Wen-Chen Xiong for the PI3K and Akt constructs, Yu-Tian Wang for the Dynamin constructs, and Regeneron Pharmaceuticals for recombinant NT-3. We also thank members of the Lu laboratory, particularly Newton Woo and Jay Chang, for the thoughtful comments and suggestions on this manuscript.

*H.-S.J. and J.Z. contributed equally to this work.

Correspondence should be addressed to Dr. Bai Lu, Chief, Section on Neural Development and Plasticity, Porter Neuroscience Research Center, Laboratory of Cellular and Synaptic Neurophysiology, National Institute of Child Health and Human Development, National Institutes of Health, Building 35, Room 1C1004 Office, MSC 3714, 35 Lincoln Drive, Bethesda, MD 20892-3714. E-mail: bailu@mail.nih.gov.

DOI:10.1523/JNEUROSCI.4087-05.2005

 0270-6474/05/2511719-11$15.00/0

tion of Akt, a downstream kinase of PI3K pathway, and new protein synthesis. All three are required for long-term, but not for acute, synaptic modulation by NT-3. Together, these results reveal mechanistic distinctions between acute- and long-term forms of neurotrophic regulation and suggest general principles that govern long-term regulation of synapses by neurotrophins.

## Materials and Methods

*DNA constructs, embryo injection, and* Xenopus *nerve-muscle coculture.* Dominant-negative (DN) Dynamin construct contains a K44E point mutation in the GTP binding domain of Dynamin and an HA tag at the N-terminal and were gifts from Dr. Yu-Tian Wang (University of British Columbia, Vancouver, British Columbia, Canada). Dominant-negative form of PI3K was made as described previously (Yang et al., 2001). The dominant-negative Akt, DN-Myc-Akt [K179M], and wild-type Akt, WT-Myc-Akt, expression vectors were kind gifts from Dr. W. Xiong (Medical College of Georgia, Augusta, GA) (Eves et al., 1998). cDNAs were digested and subcloned into an expression vector pcDNA3(+) (Invitrogen, Carlsbad, CA), which contains a T7 promoter for *in vitro* transcription of sense mRNAs. Capped mRNAs were generated by using the mMESSAGE mMACHINE kit (Ambion, Austin, TX) (Wang and Poo, 1997). *Xenopus* egg laying was induced by injecting female *Xenopus* with human chronic gonadotropin (Sigma, St. Louis, MO). Resulting eggs were fertilized artificially with sperms derived from male testis. mRNAs for NT-3, dominant-negative forms of Dynamin, PI3K, or Akt were mixed with GFP mRNA (1 $\mu$g/$\mu$l) in a 1:1 ratio. Approximately 6–12 nl of the solution was injected into one blastomere at the two- or four-cell embryonic stage using the Picospritzer pressure ejector (Parker Hannifin, Fairfield, NJ). One day after injection, the neural tube and associated myotomal tissues were dissected and used to prepare nerve-muscle cultures. Neural tube and associated myotomal tissue of *Xenopus* embryos at stage 20 were dissociated in $Ca^{2+}$-$Mg^{2+}$-free medium (58.2 mM NaCl, 0.7 mM KCl, 0.3 mM EDTA, pH 7.4) for 15–20 min. Cells were plated on clean glass coverslips and grown in the presence or absence of NT-3 (2 nM; gift from Regeneron Phamaceuticals, Tarrytown, NY) for 2 d at room temperature, as described previously (Wang et al., 1995). The culture medium consisted (v/v) of 50% L-15 medium, 1% fetal calf serum, and 49% Ringer's solution (117.6 mM NaCl, 2 mM $CaCl_2$, 2.5 mM KCl, 10 mM HEPES, pH 7.6). Various inhibitors and NT-3 were added to the cultures 6 h after plating, when cells were completely settled.

*Electrophysiology.* Synaptic currents were recorded from innervated muscle cells in 1- or 2-d-old cultures by the whole-cell recording method in culture medium at room temperature (Wang et al., 1995). The internal pipette solution contained 150 mM KCl, 1 mM NaCl, 1 mM $MgCl_2$, and 10 mM HEPES buffer, pH 7.2. The membrane potentials of the muscle cells recorded were generally in the range of −55 to −75 mV and were voltage clamped at −70 mV. To elicit evoked synaptic currents (ESCs), square current pulses (0.5–1 ms, 0.5–5 V) were applied with a patch electrode filled with Ringer's solution at the neuronal soma under loose seal conditions. All data were collected by an Axopatch 200B patch-clamp amplifier (Molecular Devices, Foster City, CA), with a current signal filter set at 3 kHz. Spontaneous synaptic current (SSC) frequency is defined as the number of SSC events per minute. The amplitudes of SSCs and ESCs were analyzed using SCAN software (Dagan, Minneapolis, MN). Pipette and membrane capacitance and serial resistance were compensated. All recordings of SSCs were done in the presence of tetrodotoxin (TTX; 1 $\mu$M). For acute effect, data are presented as normalized SSC frequency for two reasons. First, we compared the effect before and after NT-3 application on the same cell. Second, the data from 1-d-old cultures are usually more variable than those from 2-d-old cultures. For long-term effect, data from different cells were compared, allowing presentation of the actual SSC frequency.

*FM 1–43 imaging.* For FM-dye imaging, the fluorescent styryl membrane dye, FM 1–43 (Invitrogen, Eugene, OR), was loaded into *Xenopus* spinal neurons by applying high $K^+$ loading solution (60 mM KCl, 57.6 mM NaCl, 3.5 mM $CaCl_2$, 10 mM HEPES, pH 7.6; FM 1–43, 2 $\mu$M) to control or NT-3-treated cultures for 2 min. Cells were then rinsed extensively with Ringer's solution to remove membrane bound FM-dye. Then, fluorescent images of FM-dye were acquired by a MicroMax 1300 cool CCD camera (Roper Scientific, Trenton, NJ) mounted on an Olympus IX70 inverted epifluorescence microscope and analyzed off-line using IPLab software (Scanalytics, Fairfax, VA). Fluorescence images were taken with 1000 ms exposure time with a 40×, 0.55 numerical aperture (NA) objective. The pseudocolor (green) was assigned to fluorescent images, and the superimposed Hoffman optics and fluorescence images were created by the IPLab software. FM-dye destaining experiments were performed as described previously (Ryan et al., 1993) with minor modification. In brief, FM 1–43 was loaded into neurons as described above for 3 min, and cells were washed extensively with Ringer's solution. Fluorescence images were acquired at a rate of 0.2 Hz with 250 ms exposure time with a 25×, 0.4 NA objective. After acquiring five images (10 s) as a baseline, FM 1–43 destaining was initiated by rapid perfusion of high $K^+$ loading solution (60 mM KCl, 57.6 mM NaCl, 2.0 mM $CaCl_2$, 10 mM HEPES, pH 7.6). The image data were stored and analyzed off-line by IPLab software. Fluorescence intensities were extracted from time-lapse images of individual boutons. The data were normalized to background fluorescence, fitted by single exponential curves, and time constants ($\tau$) were obtained and averaged.

*Quantification of FM-dye fluorescence image.* Each pixel in a fluorescent image contains intensity information that follows a normal distribution around the peak intensity. To obtain the number of fluorescence spots, an arbitral threshold is usually placed on fluorescent signals across the entire image, and the number of spots that pass this intensity threshold was counted. However, this analysis cannot be used to accurately measure the intensity information. To quantify the intensity of fluorescent spots, a common way is to use the same size of windows or region of interests (ROIs) on each fluorescent spot (Ryan et al., 1996). This analysis, although revealing the true intensity value for each is to fluorescent signal, is difficult to obtain the true number of the fluorescent spots. To truthfully reflect the changes in the number as well as the intensity of the fluorescent varicosity and yet to avoid cumbersome data presentation, we used a morphological index that combined two quantification measurements with equal weights (morphological index, 0.5 × number of fluorescent spot per unit length of axon + 0.5 × average fluorescence intensity of fluorescent spots in axon) (McAllister et al., 1995). To measure the number of fluorescent spots, we first calculated background intensity by averaging intensities from three nonfluorescent areas along the axon. To eliminate nonspecific fluorescent signals, a fluorescent spot was considered as a "varicosity" only when the following criteria were met: (1) its average fluorescent intensity was higher than 100% above the background; and (2) its size was larger than 0.5 $\mu$m in diameter. By using the ROI tool in the IPLab program, the number of fluorescent spots in the axon and the length of neuronal process were calculated in a semiautomated way. The number of fluorescent spots in 100 $\mu$m was calculated by the following formula: total number of spots/total length of axon × 100 $\mu$m = the density of fluorescent spots. To measure unbiased average intensity of the fluorescent spots, we first measured the optical center of mass of a given fluorescent spot. Then, we placed the same size of ROI (0.5 × 0.5 $\mu$m) to the center of mass of each fluorescent spot and measured the intensity of each spot. Then, measured intensity of spots in a single neuron were pooled and averaged. Student's *t* test was used for statistical analysis.

*Western blotting. Xenopus* embryos at stage 20 were quickly homogenized in extraction buffer (100 mM NaCl, 50 mM Tris-HCl, pH 7.5, 1% NP-40, 2 mM PMSF, 1 $\mu$g/ml aprotinin, 1 $\mu$g/ml leupeptin, 1 $\mu$g/ml pepstatin A, 2 $\mu$M $Na_3VO_4$) and subsequently sonicated. High-speed centrifugation produced an insoluble pellet that was discarded. Supernatants were transferred to a fresh tube containing 300 $\mu$l of Freon (1,1,2-trichlorotrifluoroethane) (Sigma) vortexed for 1 min, incubated on ice for 5 min, and centrifuged again to remove yolk protein. The protein concentrations of the supernatants were determined using the Bio-Rad (Hercules, CA) protein assay. The proteins were separated by SDS-polyacrylamide electrophoresis and blotted onto Immobilon-P membrane (Millipore, Bedford, MA). The blots were probed with primary antibodies (anti-HA for Dynamin, 1:200; anti-c-myc for PI3K or Akt, 1:300), followed by a secondary antibody conjugated with HRP. Signals were detected by chemiluminescence kit (Pierce, Rockford, IL).

*Immunofluorescence microscopy.* *Xenopus* nerve-muscle cultures were treated with or without pharmacological drugs for 30 min at room temperature before NT-3 application. The cultures were fixed 30 min after NT-3 application by using 4% paraformaldehyde (EM Science, Gibbstown, NJ) for 30 min at room temperature and washed three times with 0.1 M $NaBH_4$ (sodium borohydrate) in PBS to reduce autofluorescence. Fixed cells were permeabilized with 0.1% Triton X-100 in PBS for 5 min. Fixed cells were blocked with 5% BSA and incubated with primary antibodies against phospho-Akt 1:100 (polyclonal; Cell Signaling Technology, Beverly, MA) or phospho-ribosomal S6 protein 1:200 (polyclonal; Cell Signaling Technology) overnight at 4°C. Secondary antibodies were Alexa 546 (Invitrogen). Fluorescent images were captured with an Olympus (Tokyo, Japan) IX70 microscope using a CCD camera, acquired with IPLAb software and processed with Adobe Photoshop (Adobe Systems, San Jose, CA). For statistical analysis, >70 neurons (see Fig. 7) or >20 neurons (supplemental Fig. 4, available at www.jneurosci.org as supplemental material) from at least three different experiments were measured. The $\chi^2$ test was used to determine the level of significance.

*Preparation of NT-3-bead.* Generation of NT-3-beads is based on a noncovalent but very tight binding interaction between streptavidin and biotin. To biotinylated NT-3 in mild physiological condition, FluoReporter Biotin-XX protein labeling kit was used (Invitrogen). Briefly, 100 μg of NT-3 was diluted with 200 μl of distilled water and 20 μl of 1 M sodium bicarbonate (0.84 g of $NaHCO_3$ in 10 ml of distilled water; pH 8.4) was added. Two microliters of reactive form of Biotin-XX and sulfosuccinimidyl ester sodium salt were added into a reaction tube that contained NT-3 in bicarbonate solution and incubated for 2 h at room temperature. After biotinylation, NT-3-biotin was collected and purified by a spin column. Approximately 80–90% of biotinylated NT-3 is recovered after column centrifugation. The biological activity of NT-3-biotin was accessed by electrophysiological recording. To quantify biotinylated NT-3, we measured the protein concentration of biotin-labeled NT-3 by analyzing the absorbance at 280 nm using a NanoDrop spectrophotometer (Nanodrop Technology, Wilmington, DE), because biotin does not absorb at 280 nm. Then, the number of biotin labels on a protein was determined by using the biotin quantification assay kit (Invitrogen). To make NT-3-bead, 100 μl of streptavidin beads (1.25% w/v; Bangs Laboratories, Fisher, IN) with binding capacity of 7.5 μmol biotinylated conjugates per 1 μl of bead were rinsed three times with PBS, centrifuged, and resuspended in 100 μl of 0.1 M PBS, pH 7.4. To this, 100 μg of freshly made NT-3-biotin was added and allowed to mix on a rotary shaker overnight (12–14 h) at 4°C. NT-3-beads were centrifuged and rinsed three times to remove any unbound NT-3-biotin. The pelleted NT-3-beads resuspended in 100 μl of 0.1 M PBS and stored at 4°C until use. To quantify amounts of NT-3 on NT-3-bead, we deduced the approximate concentration of NT-3 biotin from the number of beads per milliliter ($2.5 \times 10^{11}$ particles/ml) and the amounts of proteins bound. NT-3 bound to each bead was estimated to be 0.30 ± 0.05 pg ($n = 3$). By electrophysiological measurement, we found that 2 μl of beads in PBS (30 ng of NT-3 bead) was enough to induce acute synaptic potentiation in a single neuron. Therefore, we set this concentration comparable with 50 ng/ml NT-3. For long-term experiments, we used 0.2 μl of beads, which is 10 times lower, to cover each neuron. To test the strength of bond between NT-3-biotin and avidin-beads, 5 μl of NT-3 beads was vortexed for 30 s and spun for 5 min. Then, the free NT-3 in the supernatant was measured by NT-3 $E_{max}$ Immunoassay system (Promega, Madison, WI). In three independent experiments, the concentration of NT-3 in the supernatant was lower than the detection level of the kit (≪10 pg/ml).

*Protein synthesis inhibition assay.* We used destabilized EGFP vector (pd1EGFP-N1; Clontech, Cambridge, UK) to monitor the inhibition of new protein synthesis. In this vector, residues 422–461 of mouse ornithine decarboxylase (MODC) were fused to the C terminus of EGFP, and this region of MODC contains a PEST amino acid sequence that targets the protein for degradation and results in rapid protein turnover. This PEST amino acid sequence of MODC is highly conserved in *Xenopus*, mice, and humans and correlated with most short-lived proteins. pd1EGFP has a half-life of ~1 h, as measured by fluorescence intensity of cells treated with the protein synthesis inhibitor cycloheximide (Li et al., 1998). pd1EGFP was expressed in *Xenopus* spinal neurons by embryo injection. pd1EGFP-associated fluorescence for a given neuronal soma was calculated by subtracting the fluorescence intensity in background area (representing no-cell area) from the averaged intensity of three different areas. Each image was collected with time-lapse fluorescence microscopy. Average fluorescence intensity was calculated for a region of interest containing a single neuronal soma. The dimensions of each region of interest were six pixels by six pixels ($1.0 \times 1.0$ μm). Regions of interest were initially positioned by the eye and corrected for the center of mass of each soma by an automated script in IPLab. Initial average intensity from three frames was considered as 100% fluorescence intensity and fluorescence intensity from each frame was normalized to correct for possible changes in gain between experiments. Drugs (rapamycin, 200 nM) (Biomol, Plymouth meeting, PA) were added 30 min before time-lapse recording, and no adverse morphological change was observed after drug treatment.

## Results

### Physiological and morphological changes at NMJ induced by long-term treatment with NT-3

At the *Xenopus* neuromuscular synapses, application of exogenous NT-3 at a high concentration (50 ng/ml) induces a rapid potentiation of synaptic transmission within 5 min (Lohof et al., 1993), whereas long-term treatment with NT-3 (50 ng/ml; 2 d) facilitates physiological and morphological maturation of the synapses (Wang et al., 1995). To determine whether simple extension of NT-3 incubation would convert the acute to long-term effects, or the two temporally different modes of NT-3 actions operate by different mechanisms, we used a low concentration (5 ng/ml) of NT-3. At this concentration, NT-3 did not elicit acute synaptic potentiation. No physiological change was observed even when the cells were treated with NT-3 for 1 h at this concentration. The frequency of SSCs 1 h after NT-3 treatment was 97.2 ± 21.3% of that of control ($n = 6$; $p > 0.6$; *t* test). Thus, a lower dose of NT-3 did not merely delay the timing of an acute response. In contrast, long-term treatment (2 d) at this concentration resulted in a marked increase in synaptic efficacy at the neuromuscular synapses. The frequency and amplitude of SSCs were 5.2 ± 1.8 events/min and 310 ± 34 pA in untreated synapses ($n = 11$) but 13.4 ± 2.7 events/min and 489 ± 71 pA in NT-3-treated synapses ($n = 13$; $p < 0.01$ for SSC frequency; $p < 0.05$ for ESC amplitude; *t* test). All recordings of SSCs were done in the presence of TTX (1 μM), and therefore the increase was not a result of firing of action potentials or increase in neuronal excitability.

To determine whether these changes occur in a synapse-specific manner, we expressed NT-3 gene in postsynaptic muscle cells by embryo injection techniques (Wang et al., 1995). Synaptic activities were compared in a triplet system in which a spinal neuron innervated two myocytes, one of which expressed exogenous NT-3 (as indicated by GFP fluorescence) (Fig. 1*A*). The whole-cell recording was made on both myocytes in the triplet. The frequency (events/min) of SSCs was 5.8 ± 1.7 from control synapses (myocytes not expressing NT-3, or M-) but 14.3 ± 2.4 in NT-3-expressing synapses (M+) ($n = 13$ in both; $p < 0.02$; *t* test), suggesting that NT-3 increased transmitter release by approximately twofold to threefold (Fig. 1*B*). There was no change in SSC amplitude (469 ± 57 pA in M-synapses and 465 ± 60 pA in M+ synapses; $p > 0.7$; *t* test). It is unclear why postsynaptic NT-3 expression was less effective than bath application of NT-3 in changing SSC amplitude. Because the postsynaptic effect of NT-3 was relatively small, we focused our analysis on the SSC frequency.

The amplitude of ESCs, elicited by stimulating presynaptic

somata of spinal neurons, was also higher at synapses treated with exogenous NT-3 for 2 d (Fig. 1*C*). The amplitude of ESCs were 1746 ± 253 pA from myocytes not expressing NT-3 but 3263 ± 310 pA from NT-3-expressing myocytes ($n = 8$; $p < 0.01$). The rise time and decay time of ESCs were not changed (data not shown). The changes in spontaneous and evoked synaptic activities suggest that long-term postsynaptic expression of NT-3 could enhance synaptic efficacy by regulating presynaptic neurotransmitter release properties.

Next, we examined whether acute or long-term treatment with NT-3 induces any morphological change indicative of more mature synapses. Similar to cultured hippocampal neurons (Baranes et al., 1996), the axons of *Xenopus* spinal neurons exhibited "morphological varicosities" (Fig. 2*A*) that contain clusters of synaptic vesicles as well as other presynaptic elements necessary for exocytosis and endocytosis. It has been shown that in developing neurons, membrane recycling is not limited to the nerve terminal but occurs in the entire axonal surface, particularly at the varicosities (Sun and Poo, 1987; Evers et al., 1989; Dai and Peng, 1996), and spontaneous transmitter secretion along the axonal shaft is strikingly similar to that in the terminals (Chang and Popov, 1999). Moreover, synaptic varicosities have been shown to serve as synaptic boutons at the NMJ of *Drosophila* larvae and *Caenorhabditis elegans in vivo* (Davis et al., 1998; Zhao and Nonet, 2000). Thus, the number and the size of the varicosities may reflect the maturation of neurotransmitter release capacity.

To effectively reveal synaptic varicosities, we used the FM dye staining technique (Betz et al., 1992; Ryan et al., 1993; Wang et al., 2002). Cultures were exposed to high $K^+$ (60 mM) solution for 3 min in the presence of FM 1–43 (2 μM). Such depolarization elicited a massive vesicle fusion, followed by a rapid internalization of FM 1–43 dye, which labels all recycling synaptic vesicles. As shown in Figure 2*A*, strong fluorescent spots, which reflect clusters of FM-dye loaded vesicles, were observed along the axons of spinal neurons in all cultures. Synaptic varicosities are defined as morphological spots with fluorescence intensity two times or more than background and larger than 0.5 μm in diameter. Treatment of the neurons with NT-3 significantly increased the number (control, 0.69 ± 0.10 spot/100 μm; NT-3, 1.70 ± 0.22 spot/100 μm; $p < 0.02$), as well as the average fluorescent intensity (control, 2.00 ± 0.08 fluorescence unit; NT-3, 2.45 ± 0.07 fluorescence unit; $p < 0.01$) of the FM dye spots (Fig. 2*A*). Because the changes in the number and the intensity usually went in parallel, we used a morphology index (morphological index, 0.5 × number of fluorescent spot per unit length of axon + 0.5 × average fluorescence intensity of fluorescent spots in axon) for the assessment of FM dye spot (Fig. 2*B*) (see Materials and Methods). In contrast, acute application of NT-3 did not result in any morpho-

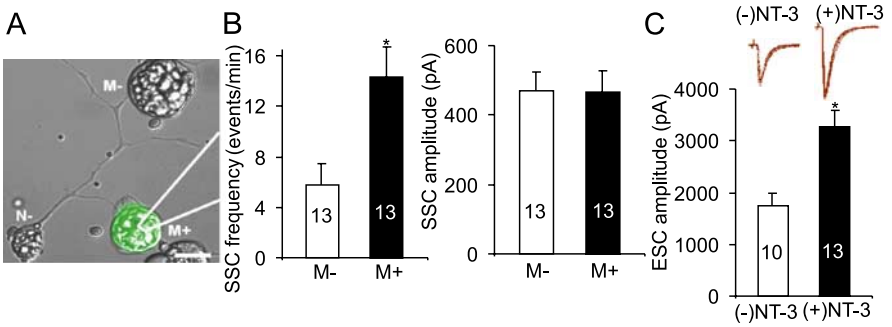


**Figure 1.** Physiological changes at *Xenopus* neuromuscular synapses induced by long-term treatment with NT-3. ***A***, A superimposed Hoffman and GFP fluorescence image showing a triplet: a motoneuron (*N*−) innervating two myocytes, one of which expresses NT-3 gene (M+), whereas the other does not (*M*−). The NT-3 gene was introduced into the system through embryo injection. The expression of NT-3 gene is indicated by GFP fluorescence. ***B***, Quantitative analysis of the frequency and amplitude of SSCs recorded from synapses made by myocytes expressing NT-3 (M+) and paired synapses made by myocytes not expressing NT-3 (*M*−). ***C***, Effect of NT-3 on ESCs. *Xenopus* nerve-muscle cultures were treated with NT-3 for 2 d. ESCs were elicited by stimulating neuronal soma. Inset, Superimposed traces of ESCs in control and NT-3-treated synapses. In this and all other figures, data are presented as mean ± SEM. The number associated with each column represents the number of cells analyzed. In all figures, the asterisks indicate significantly higher than the respective "NT-3 (−)" group, by statistical test ( $p < 0.05$). Error bars represent SEM.

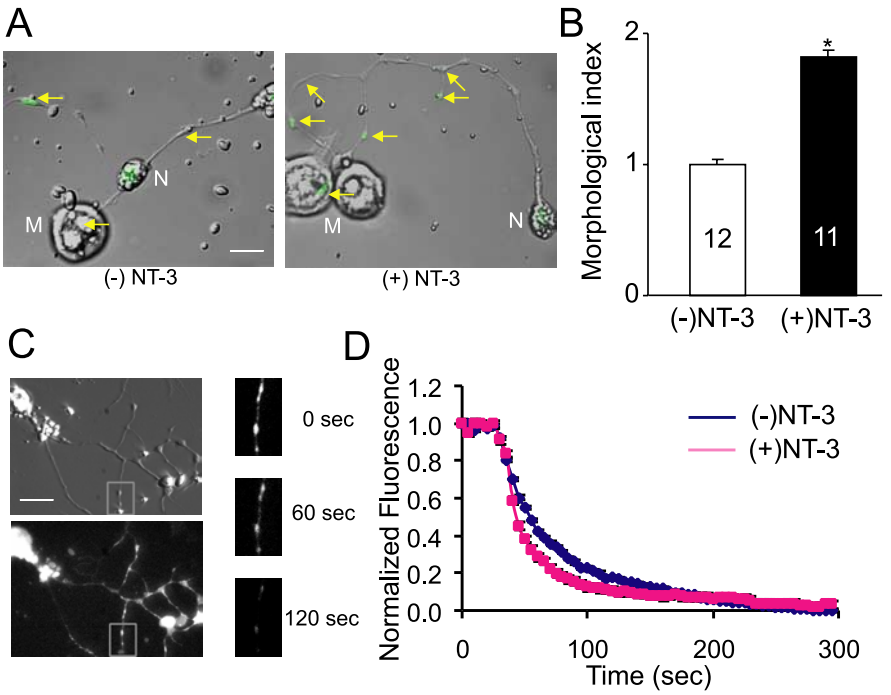


**Figure 2.** Morphological changes at *Xenopus* neuromuscular synapses induced by long-term treatment with NT-3. ***A***, ***B***, Effect of NT-3 on synaptic varicosities, visualized by FM dye. FM dye was loaded into spinal neurons by a brief exposure (2 min) to high $K^+$ (60 mM) Ringer's solution, followed by extensive washes. ***A***, Superimposed Hoffman and fluorescence images of FM dye-labeled neurons in control and NT-3-treated (5 ng/ml; 48 h) cultures. Yellow arrows indicate FM-labeled synaptic varicosities. M, Myocytes; N, neurons. Scale bar, 20 μm. ***B***, Morphological index showing changes in total quantity of recycling synaptic vesicle pool in NT-3-treated spinal neurons. ***C***, ***D***, Effect of NT-3 on FM 1–43 destaining. ***C***, Images of a neuron loaded with FM 1–43 dye in phase (top left) and fluorescence (bottom left). Three images are magnified to visualize FM dye-labeled varicosities with different time periods (before unloading, after 60 s, and after 120 s). Note that after application of high $K^+$ destaining solution, FM-dye-labeled varicosities lost most of their contents within 2 or 3 min. ***D***, Averaged destaining curves. After FM 1–43 loading, the cells were rinsed extensively with wash solutions. The error bars are too small to be visualized.

logical change (data not shown). Thus, long-term exposure to NT-3 may facilitate the formation of synaptic vesicle clusters and increase the numbers of release sites.

To confirm that these FM dye-labeled varicosities truly reflect synaptic release sites, we performed FM dye destaining experiments. Figure 2*C* shows the images of a spinal neuron loaded with FM 1–43. Strong fluorescence was observed in the synaptic varicosities. Transmitter release was initiated by rapid perfusion of high $K^+$ destaining solution containing the same $[Ca^{2+}]_o$ (2 mM) as the wash solution. More than 90% of the dye fluorescence disappeared within 2 min after the perfusion of high $K^+$ destaining solution (Fig. 2*D*) (supplemental movie, available at www.jneurosci.org as supplemental material). The time constant ($\tau$) was 43.2 ± 4.2 s in control neurons ($n = 16$) and 29.8 ± 5.3 s in neurons treated with NT-3 for 2 d ($n = 13$; $p < 0.04$; *t* test). We also analyzed destaining kinetics from FM dye-labeled spots within postsynaptic myocytes, which presumably serve as sites for synaptic vesicle release. The time constant was 57.4 ± 8.2 s in control synapses ($n = 9$) and 28.4 ± 5.6 s in synapses treated with NT-3 for 2 d ($n = 7$; $p < 0.05$; *t* test). These data are consistent with the changes in SSC frequency. Together, these results suggest that long-term exposure to NT-3 not only enhances transmitter release but also promotes the morphological differentiation of the synaptic boutons.

### Requirement of endocytosis of NT-3 receptor complex in NT-3-mediated long-term synaptic effects

After binding and activation of the Trk receptors, the neurotrophin-receptor complex gets endocytosed (Grimes et al., 1996). To determine whether the endocytosis of NT-3-receptor complex is necessary for acute and/or long-term synaptic modulation, we introduced two forms of Dynamin I in spinal neurons through embryo injection. Dynamin I is the GTPase required in the final step of endocytosis. We used DN Dynamin I, in which lysine 44 is replaced with glutamate (K44E), to block endocytosis. Western blot analysis revealed the expression of either HA-tagged WT or DN-Dynamin in 2-d-old embryos, suggesting that the injected mRNAs remained intact at the time of electrophysiological recording (Fig. 3*A*). In 1-d-old cultures, acute application of NT-3 elicited a marked increase in transmitter release in neurons expressing DN-Dynamin (Fig. 3*B*). Thus, inhibition of endocytosis does not affect the acute modulation of transmission by NT-3. In contrast, expression of DN-Dynamin in presynaptic neurons completely blocked the enhancement of synaptic efficacy induced by long-term exposure to NT-3 (Fig. 3*C*). In DN-Dynamin-expressing synapses, the SSC frequency was 3.14 ± 0.5 events/min in the absence of NT-3 ($n = 11$), but NT-3 treatment no longer increased SSC frequency (3.7 ± 0.52 events/min; $n = 19$; $p > 0.5$; *t* test). Expression of WT-Dynamin did not prevent the potentiating effect of NT-3 (control, 5.7 ± 0.8 events/min; NT-3, 12.8 ± 0.9 event/min; $p < 0.05$; *t* test) (Fig. 3*C*). Moreover, expression of DN-Dynamin in the postsynaptic muscle cells (N-M+) had no effect on NT-3-induced synaptic potentiation (control, 5.8 ± 0.7 events/min; NT-3, 13.8 ± 0.6 events/min; $p < 0.05$; *t* test) (Fig. 3*C*). Almost identical results were obtained using the amplitude of ESCs to measure synaptic efficacy. Expression of DN-Dynamin in presynaptic neurons completely prevented the potentiating effect of NT-3 on ESC amplitude (control, 855 ± 147 pA; NT-3, 635 ± 176 pA; $p > 0.4$; *t* test) (Fig. 3*D*). These results support the notion that endocytosis of NT-3-TrkC complex in presynaptic neurons is important for NT-3-induced long-term, but not acute, synaptic modulation.

One may argue that DN-Dynamin could also affect the endocytosis of vesicles for neurotransmitter or factors other than NT-3; therefore, expression of DN-Dynamin prevented the effect of NT-3. Indeed, there was a small but significant reduction (30–40%) in basal SSC frequency (control, 6.1 ± 0.6 event/min; DN-Dynamin, 3.1 ± 0.5 events/min; $p < 0.05$) and ESC amplitude (control, 1746 ± 253 pA; DN-Dynamin, 855 ± 147 pA; $p < 0.05$) recorded in untreated DN-Dynamin-expressing neurons (Fig. 3*C*,*D*). Two experiments were performed to address this concern. First, we reasoned that if the expression of DN-dynamin affects the general well being of transmitter release properties, then the acute synaptic modulation by NT-3 should not occur in 2-d-old culture. However, the acute effect persisted even in neurons expressing DN-Dynamin for 2 d (supplemental Fig. 2*B*, available at www.jneurosci.org as supplemental material), suggesting that inhibition of endocytosis for 2 d does not alter the basic transmitter release properties.

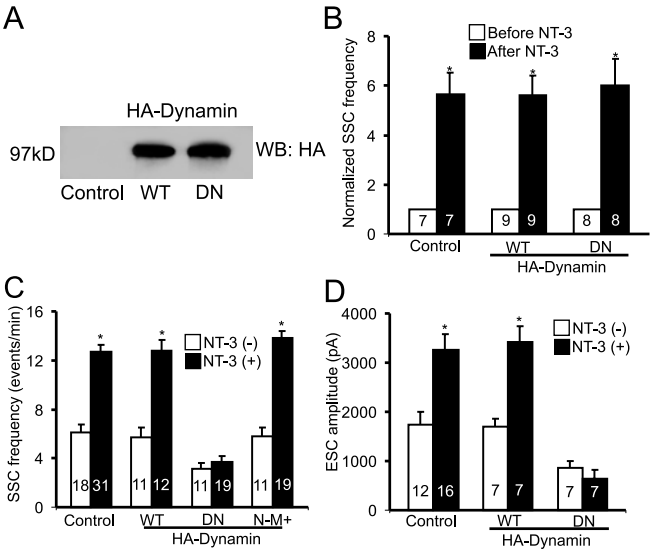


**Figure 3.** Blockade of long-term NT-3 effect by presynaptic expression of dominant-negative Dynamin. ***A***, An immunoblot showing the expression of HA-tagged WT or DN-Dynamin (probed with anti-HA antibody) in 1-d-old *Xenopus* embryos. ***B***, Inhibition of endocytosis by DN-Dynamin does not prevent acute potentiation of synaptic transmission by NT-3. Summary of effect of acute NT-3 application on uninjected control synapses, synapses with presynaptic WT-Dynamin, or DN-Dynamin expression. Each data set represents the frequency of SSCs (averaged from 10 min of recording) from a single synapse before and after NT-3 application. ***C***, ***D***, Presynaptic inhibition of endocytosis prevents NT-3-induced long-term potentiation of SSC frequency (***C***) and ESC amplitude (***D***). WT, WT-Dynamin expressed presynaptically; DN, DN-Dynamin expressed presynaptically; N-M+, DN-Dynamin expressed postsynaptically. Error bars represent SEM.

Second, we tested the acute and long-term effects of NT-3-biotin–avidin conjugated beads (NT-3-beads) that were too large (>1 μm in diameter) to be internalized into neurons or muscle cells (Fig. 4*A*). Briefly, recombinant NT-3 was biotinylated (NT-3-biotin) and incubated with avidin-conjugated beads (Avidin-bead), which was conjugated with cyanine 3 and therefore emitted a red fluorescence. Unbound biotinylated NT-3 was removed by extensive washes. The bond between NT-3-biotin and avidin-beads should be extremely tight and, therefore, there should be no free or biotinylated NT-3. To test this, 5 μl of NT-3 beads were vortexed for 30 s and spun for 5 min. In three independent experiments, the free NT-3 in the supernatant, measured by ELISA, was lower than detection level (<10 pg/ml).

Both acute and long-term effects of the NT-3-beads were tested. Two microliters of NT-3-bead (30 ng) were sufficient to induce maximal acute potentiation (Fig. 4*B*). For long-term

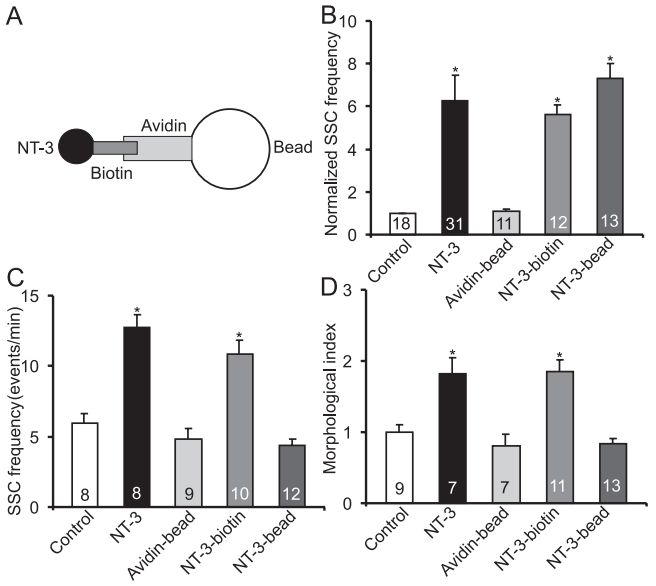


**Figure 4.** Failure to elicit long-term synaptic modulation by NT-3-beads. ***A***, Schematic diagram for NT-3-beads. ***B***, Acute effect of NT-3 beads on synaptic transmission. For each synapse, averaged SSC frequencies from a 10 min recording after application of various agents were normalized to those before application of the agents. NT-3-beads increased the frequency of SSCs at the neuromuscular synapses, just as NT-3 and NT-3-biotin. ***C***, Effect of long-term treatment on synaptic efficacy. Cultures were treated with indicated agents for 48 h. Unlike NT-3 and NT-3-biotin, NT-3-beads failed to facilitate synaptic efficacy. ***D***, Effect of long-term treatment on synaptic morphology. The cultures treated the same way as in ***C*** were processed for FM dye labeling, and labeling index is presented. Unlike NT-3 and NT-3-biotin, NT-3-beads failed to increase synaptic varicosity. Error bars represent SEM.

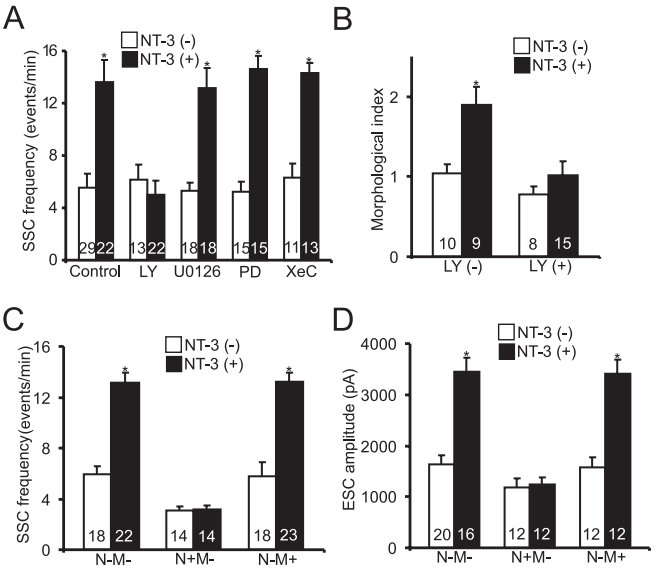


**Figure 5.** Requirement of PI3 kinase in the long-term synaptic action of NT-3. ***A***, Pharmacological characterization of signaling pathways involved in NT-3-induced long-term synaptic modulation. Cultures were treated with or without NT-3 and various inhibitors for 2 d: PD098059 (PD; 10 $\mu$M) or U0126 (5 $\mu$M) for MAP kinase, LY294002 (LY; 5 $\mu$M) for PI3K, XeC (1 $\mu$M) for $IP_3$ receptors. SSC frequencies were averaged from 20 min of recording. ***B***, Blockade of NT-3-induced changes in synaptic varicosity by inhibition of PI3K. Cultures were pretreated with LY294002 before NT-3 application. ***C***, ***D***, Effect of DN-PI3K on SSC frequency (***C***) and ESC amplitude (***D***). DN-PI3K was expressed in spinal neurons (N+), myocytes (M+), or neither (N-M-) through embryonic injection. Error bars represent SEM.

treatment, we used one-tenth of the amount used for acute effect or 3 ng (0.2 $\mu$l of NT-3 beads in PBS) of NT-3 beads. Interestingly, long-term treatment of the cultures with the NT-3-beads no longer elicited any change in synaptic efficacy (control, 5.9 ± 0.7 events/min; NT-3 bead, 4.4 ± 0.4 events/min; $p > 0.2$; $t$ test) (Fig. 4*C*). As controls, treatment with NT-3-biotin induced similar magnitude of synaptic potentiation as NT-3 alone (10.9 ± 0.9 events/min; $p < 0.05$; $t$ test), and treatment with avidin-beads had no effect (4.8 ± 0.8 events/min) (Fig. 4*C*). Moreover, NT-3-beads did not induce any long-term change in synaptic varicosities (Fig. 4*D*). It was also noted that the biological activity of the NT-3 conjugated beads was stable over 2 d in culture medium at room temperature. Together, endocytosis of the NT-3-receptor complex is required for the long-term physiological and morphological development of the neuromuscular synapse.

### Critical role of Akt in NT-3-mediated long-term synaptic effects

We have demonstrated previously that activation of PI3K and PLC-$\gamma$ signaling pathways is both necessary and sufficient to mediate the acute synaptic potentiation induced by NT-3 (Yang et al., 2001). To test whether PI3K is also involved in long-term modulation of NMJ by NT-3, we applied 2-(4-morpholinyl)-8-phenyl-4H-1-benzopyran-4-one (LY294002; 5 $\mu$M) (Vlahos et al., 1994), a specific inhibitor of PI3K. Although this inhibitor did not produce any change at control synapses, cotreatment with NT-3 and LY294002 for 2 d blocked NT-3-induced synaptic potentiation in terms of SSC frequencies (control, 5.6 ± 1.0 events/min; LY294002, 6.1 ± 1.2 events/min; NT-3, 13.7 ± 1.7 events/min; LY294002 with NT-3, 5.0 ± 1.0 events/min) (Fig. 4*A*). Treatment with another PI3K inhibitor, wortmannin (100 nM) (Powis et al., 1994), also prevented the NT-3-induced increase in SSC frequency (data not shown). In contrast, inhibition of MAP kinase pathway by either 2′-amino-3′-methoxyflavone (PD098059) (10 $\mu$M) (Alessi et al., 1995) or 1,4-diamino-2,3-dicyano-1,4-*bis*(2-aminophenylthio)butadiene (U0126) (10 $\mu$M) (Zhu et al., 2002) did not abolish the NT-3-induced increase in SSC frequency (U0126, 5.3 ± 0.6 events/min; PD098059, 5.2 ± 7.8 events/min; U0126 with NT-3, 13.1 ± 1.6 events/min; PD098059 with NT-3, 14.6 ± 1.0) (Fig. 5*A*). Treatment with Xestospongin C (XeC) (1 $\mu$M) (Gafni et al., 1997), a specific inhibitor for $IP_3$ receptor, also had no effect on NT-3-induced synaptic potentiation (XeC, 6.4 ± 1.0 events/min; XeC with NT-3, 14.3 ± 0.8 events/min). Thus, unlike the acute effect, the long-term modulation of NMJ development by NT-3 requires the activation of one of the three Trk signaling pathways, the PI3K pathway. To investigate the locus of PI3K action, we expressed dominant-negative PI3K (DnPI3K) in either presynaptic spinal neurons or postsynaptic myocytes using the embryo injection techniques as described previously (Yang et al., 2001). Expression of DnPI3K in presynaptic neurons, but not in the postsynaptic myocytes, completely blocked the synaptic potentiation by NT-3 on both SSC frequency (control, 3.1 ± 0.3 events/min; NT-3, 3.1 ± 0.4 events/min) (Fig. 5*C*) and ESC amplitude (control, 1188 ± 165 pA; NT-3, 1239 ± 141 pA) (Fig. 5*D*). Similar to the physiological effects, inhibition of PI3K by LY294002 also blocked the change in synaptic varicosities induced by long-term treatment with NT-3 (Fig. 5*B*). These results suggest that both physiological and morphological changes induced by NT-3 are mediated by activation of PI3K in presynaptic spinal neurons.

A major downstream target of PI3 kinase is the serine/threonine kinase Akt. We have previously shown that Akt at the presynaptic spinal neurons could be activated by NT-3 treatment (Yang et al., 2001). Here, we tested whether Akt is required for NT-3-induced synaptic potentiation using embryo injection

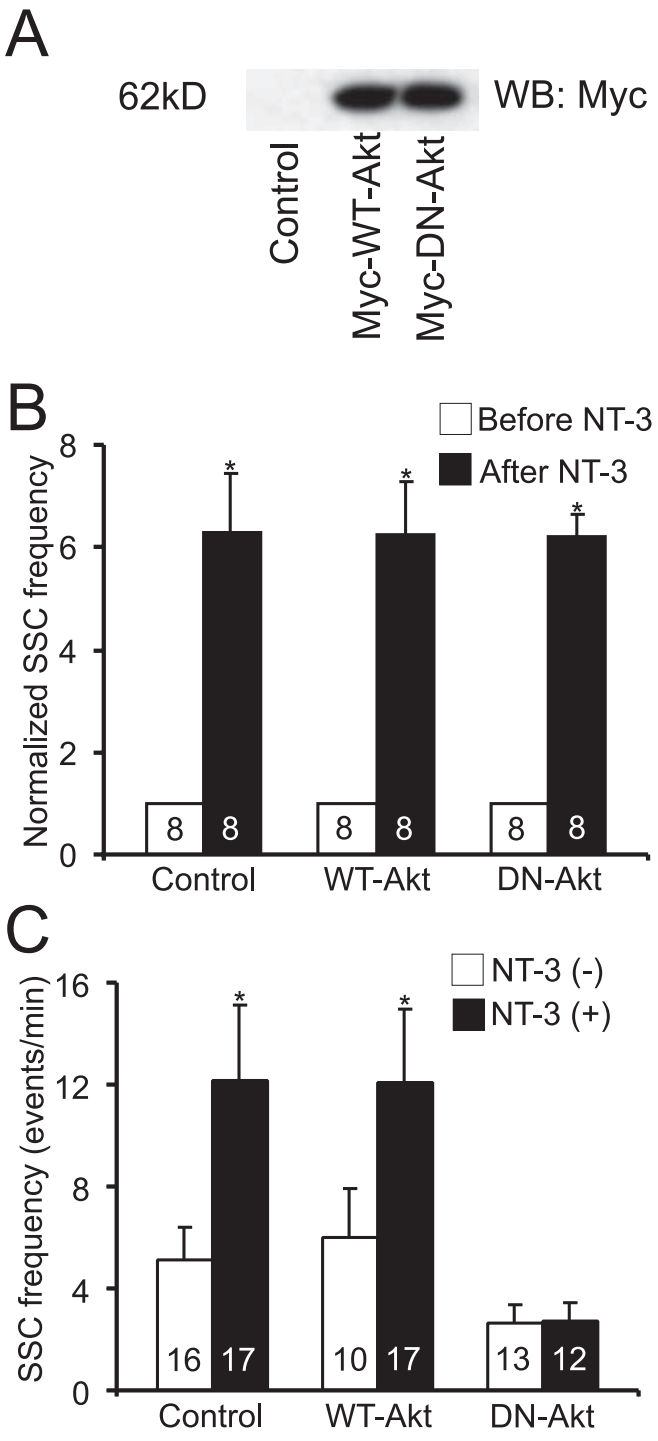


**Figure 6.** Requirement of Akt in NT-3-induced long-term synaptic modulation. ***A***, Western blot showing the expression of Myc-tagged wild-type and dominant-negative Akt (Myc-WT-Akt and Myc-DN-Akt) (probed with anti-myc antibody) in *Xenopus* neural tubes 24 h after mRNA injection. ***B***, Role of Akt in acute synaptic potentiation by NT-3. WT-Akt or DN-Akt was expressed in presynaptic spinal neurons. SSCs frequencies from a 10 min recording after application of NT-3 were normalized to those before application. ***B***, ***C***, Control, Synapses that expressed no exogenous gene. ***C***, Role of Akt in long-term modulation by NT-3, WT-Akt, or DN-Akt was expressed in presynaptic neurons. Error bars represent SEM.

techniques. Western blot analysis showed the expression of Myc-tagged wild-type and dominant-negative-Akt [Myc-WT-Akt and Myc-DN-Akt (K179M), respectively] in *Xenopus* neural tubes 2 d after embryonic mRNA injection (Fig. 6*A*). To test whether Myc-DN-Akt successfully inhibits Akt signaling, we performed immunocytochemistry using an antibody against the phosphorylated form of S6 (pS6), a ribosomal protein downstream of Akt signaling. At least 20 neurons were examined in each condition, and consistent results were obtained. Approximately 34% (9 of 26) of cells were positive for pS6 immunostaining under control conditions. Application of NT-3 increased pS6 by ~65% (15 of 23) (between with NT-3 and without NT-3; $p < 0.05$; $\chi^2$ test) (supplemental Fig. 4, available at www.jneurosci.org as supplemental material). Expression of Myc-DN-Akt in *Xenopus* spinal neurons attenuated the NT-3-induced S6 phosphorylation: ~33% (7 of 21) of cells were positive for pS6 (EGFP vs EGFP+DN-Akt, $p > 0.8$; EGFP with NT-3 vs EGFP+DN-Akt with NT-3, $p < 0.05$; EGFP+DN-Akt vs EGFP+DN-Akt with NT-3, $p > 0.9$; $\chi^2$ test) (supplemental Fig. 4, available at www.jneurosci.org as supplemental material). Neurons expressing GFP alone or noninjected control neurons still exhibited an increase in pS6 when treated with NT-3 (supplemental Fig. 4*B*,*C*, available at www.jneurosci.org as supplemental material).

Expression of Myc-DN-Akt, but not Myc-WT-Akt, in presynaptic neurons completely blocked the long-term synaptic potentiation by NT-3 on SSC frequency (DN-Akt, 2.6 ± 0.7 events/min; DN-Akt with NT-3, 2.7 ± 0.8 events/min; WT-Akt, 6.0 ± 1.9 events/min; WT-Akt with NT-3, 12.0 ± 2.9 event/min) (Fig. 6*C*). Expression of Myc-DN-Akt in postsynaptic myocytes had no effect on these synapses (data not shown). These results suggest that expression of Myc-WT-Akt alone does not produce an enhancement of long-term synaptic efficacy. Surprisingly, presynaptic expression of Myc-DN-Akt did not prevent the potentiation of synaptic transmission induced by acute application of NT-3 ( $p < 0.01$; $t$ test) (Fig. 6*B*). Thus, although both require PI3K, a major difference in the signaling mechanisms is that long-term, but not acute, synaptic modulation by NT-3 depends on the target of PI3K, Akt.

### NT-3-mediated long-term synaptic modulation requires protein synthesis

Akt is a key factor controlling protein synthesis. NT-3-induced activation of Akt results in phosphorylation and activation of the mTOR protein, leading to the initiation of protein translation (Raught et al., 2001). To test whether protein synthesis is a hallmark that sets long-term modulation by NT-3 apart from its acute effect, we used drugs that blocked protein synthesis. The two widely used protein synthesis inhibitors, anisomycin and cycloheximide, appeared to be toxic to the nerve-muscle cultures 2 d after treatment (data not shown). In contrast, 2 d treatment with rapamycin (200 nM), a specific inhibitor for mTOR, did not show any toxic effects on cultured cells (supplemental Fig. 2*F*, available at www.jneurosci.org as supplemental material). Because of a limited number of cells available in these nerve-muscle cocultures (~30 neurons per culture dish), it was not feasible to directly measure protein synthesis using conventional approaches, such as $^3$H-leucine incorporation. We therefore used two alternative approaches to measure the efficacy of rapamycin in blocking protein synthesis. First, we measured the activity of S6 kinase, an mTOR target that phosphorylates ribosomal S6 protein. Immunostaining using an anti-pS6 antibody revealed that treatment with NT-3 elicited a marked increase in pS6 in spinal neurons: ~38% (33 of 86) of cells were positive for pS6 immunostaining without treatment and 76% (86 of 113) of cells were positive after treatment with NT-3; $p < 0.01$, $\chi^2$ test) (Fig. 7*A*,*B*). This increase was severely attenuated when the cells were pretreated with rapamycin for 1 h, whereas treatment with rapamycin alone slightly reduced the basal levels of pS6: ~30% (19 of 64)

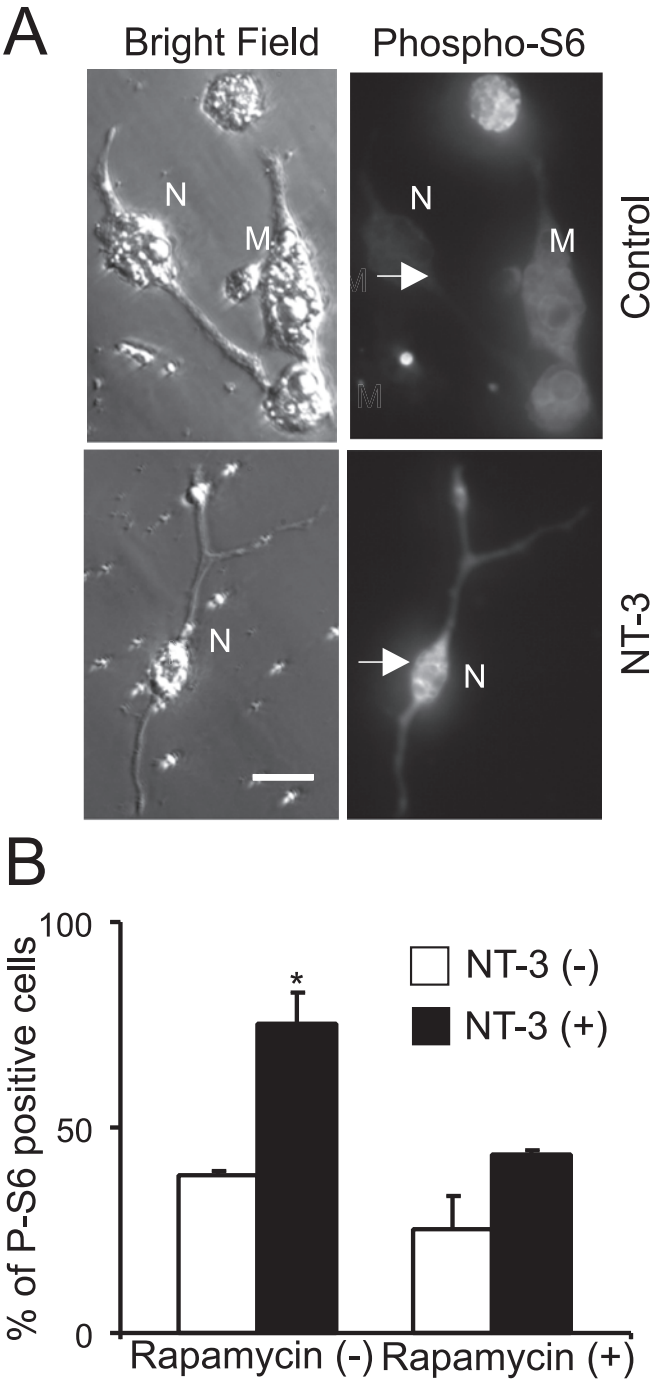


**Figure 7.** Inhibition of S6 ribosomal protein phosphorylation by rapamycin. ***A***, Sample photographs of immunohistochemistry using phospho-specific S6 protein antibody. White arrows indicate the location of the neuron. M, Myocytes; N, neurons. Scale bar, 20 $\mu$m. ***B***, Quantification of three independent experiments showing that S6 phosphorylation increases after NT-3 application and rapamycin blocks NT-3-mediated increase in S6 protein phosphorylation.

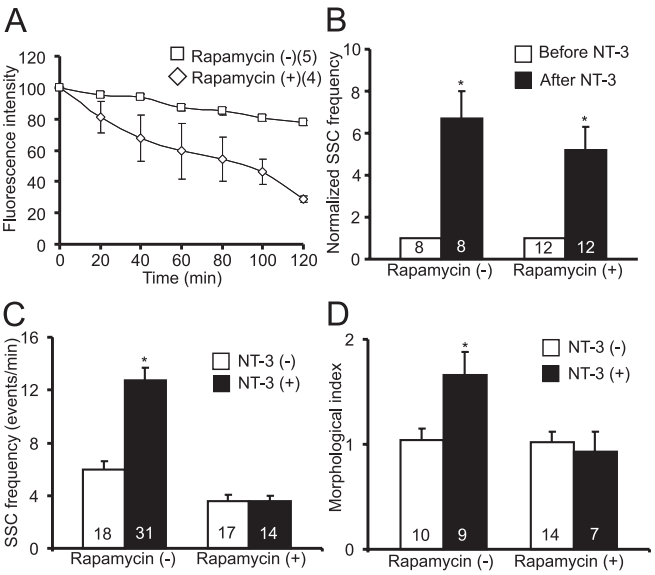


**Figure 8.** Inhibition of NT-3-induced long-term, but not acute, synaptic modulation by rapamycin. Rapamycin (200 nM) was directly applied to nerve-muscle cocultures. ***A***, Inhibition of protein translation in *Xenopus* spinal neurons by rapamycin. An unstabilized GFP (pd1-EGFP) was expressed in spinal neurons. A balance between degradation and new synthesis was normally reached such that pd1-EGFP fluorescence was maintained over time. Incubation with rapamycin for 1 h resulted in a decline of pd1-EGFP fluorescence, suggesting inhibition of protein synthesis. ***B***, Lack of effect of rapamycin on acute synaptic potentiation by NT-3. Cultures were treated with rapamycin for 1 h before application of NT-3. There was no statistical difference between the NT-3 and the rapamycin + NT-3 groups. ***C***, Blockade of NT-3-induced long-term synaptic modulation by rapamycin. ***D***, Attenuation of NT-3-induced changes in synaptic varicosity by rapamycin. Error bars represent SEM.

of cells were positive for pS6 immunostaining with rapamycin and 43% (39 of 90) of cells were positive with rapamycin and NT-3 (Fig. 7*B*). Second, we used an unstable GFP (pd1-EGFP; half life, 1 h), the fluorescence of which fades when protein synthesis is blocked. The residues 422–461 of mouse ornithine decarboxylase (MODC) were fused to the C terminus of EGFP. This region of MODC contains a PEST sequence that targets proteins for degradation, leading to a rapid protein turnover (Li et al., 1998). When pd1-EGFP was expressed in spinal neurons by embryo injection, treatment of the cultures with rapamycin (200 nM) or cycloheximide (60 $\mu$M) for 1 h greatly reduced fluorescence intensity as a result of the inhibition of new EGFP synthesis (Fig. 8*A*) (Mateus and Avery, 2000). These results confirm rapamycin successfully blocked *de novo* protein synthesis in *Xenopus* spinal neurons.

When nerve-muscle cocultures were incubated with NT-3 and rapamycin together for 2 d, the long-term effects of NT-3 on the neuromuscular synapses were abolished. As shown in Figure 8*C*, SSC frequencies exhibited no increase in synapses treated with rapamycin and NT-3 together (rapamycin, 3.6 ± 0.5 events/min; rapamycin with NT-3, 3.5 ± 0.4 events/min; $p > 0.1$; *t* test). Treatment with rapamycin alone slightly reduced the basal SSC frequency compared with control synapses (control, 5.9 ± 0.7 events/min; rapamycin, 3.6 ± 0.5 events/min) (Fig. 8*C*). Similarly, treatment with rapamycin prevented the increase in synaptic varicosities induced by long-term treatment with NT-3 without affecting the basal level of synaptic varicosity (Fig. 8*D*). In contrast, treatment with rapamycin did not affect acute potentiation of synaptic transmission elicited by 1 d or even 2 d of treatment with NT-3 (Fig. 8*B*) (supplemental Fig. 3*E*, available at www.jneurosci.org as supplemental material). Together, these data suggest that new protein synthesis is required for long-term, but not acute, synaptic effects of NT-3. To confirm that the effects of rapamycin were not attributable to nonspecific, pharmacological effects, we performed a similar analysis of SSCs, ESCs, and synaptic morphology using rapamycin at a 10 times lower concentration (20 nM). Even at this concentration, rapamycin still successfully blocked both physiological (supplemental Fig. 3*A–C*, available at www.jneurosci.org as supplemental material) and morphological (supplemental Fig. 3*D*, available at www.jneurosci.

org as supplemental material) effects by long-term treatment with NT-3.

## Discussion

Recent studies have identified neurotrophins as an important class of regulatory factors for synaptic development and plasticity. A major insight from previous studies is that neurotrophins regulate synapses in two temporally distinct modes: acute regulation of synaptic transmission and plasticity that occurs in a time scale of seconds or minutes, and long-term effects on synaptic structures and function that take days to accomplish (Lu, 2004). A number of pressing questions remain to be addressed. What are the hallmarks for the acute and long-term effects other than their temporal differences? Are two modes of actions mediated by similar or different mechanisms? We identified three characteristic features that are required for long-term, but not acute, forms of synaptic modulation by NT-3: endocytosis of neurotrophin-receptor complex, activation of Akt, and new protein synthesis. Our study provides the first systematic characterization of the mechanistic differences between two modes of neurotrophic regulation based on their distinct molecular mechanisms rather than purely on the temporal scales of their actions.

### Role of protein synthesis

Our study suggests that one of the fundamental differences between acute- and long-term forms of synaptic modulation by neurotrophins is the requirement for protein translation. To support this notion, we used rapamycin to inhibit mTOR, a kinase that phosphorylates 4E binding protein and dissociates translation factor eukaryotic initiation factor 4E. Bath application of rapamycin blocks both the physiological as well as the morphological effects induced by long-term treatment with NT-3. However, the acute effects elicited by NT-3 were not blocked by rapamycin. Consistent with this, a previous study showed that acute potentiation of synaptic transmission elicited by NT-3 is not blocked by the protein synthesis inhibitor anisomycin or cycloheximide (Chang and Popov, 1999).

NT-3-induced protein synthesis could occur in soma, presynaptic terminals, or both. Using a triplet system in which a bifurcated motor neuron innervating two postsynaptic muscle cells, one of which expressing NT-3, we found that the long-term synaptic potentiation occurred only at the NT-3-expressing synapse (Fig. 1*A*). Similar synapse-specific long-term effects were observed in a triplet system expressing NT-4 (Wang et al., 1998). These results raise the possibility that protein synthesis required for the long-term synaptic effects induced by neurotrophins occurs locally in the presynaptic terminals. Indeed, localized synaptic potentiation by BDNF has been shown to depend on local protein synthesis in the developing axons (Zhang and Poo, 2002). In *Aplysia*, local protein synthesis is thought to be a key mechanism for synapse-specific long-term facilitation induced by serotonin (Martin et al., 1997). Additional studies are necessary to determine whether such local protein synthesis contributes to the synapse specificity of neurotrophic regulation.

### Role of Akt

Although Akt is highly expressed in the CNS and is known to mediate diverse biological responses, the role of Akt in synaptic modulation has not been adequately addressed. The present study provides physiological evidence that Akt is selectively involved in long-term, but not acute, synaptic modulation. What does Akt do to contribute selectively to the long-term synaptic modulation by NT-3? Activation of PI3K occurs at the plasma membranes, whereas activated Akt acts in the cytoplasm. The cytoplasmic targets of Akt, therefore, should be considered as candidates mediating the long-term synaptic effects of NT-3. Because expression of dominant-negative Akt did not appear to affect the survival of spinal neurons (H.-S.J. and B.L., unpublished observation), it is less likely that conventional targets of Akt such as Bcl-2-associated death protein, Forkhead, or nuclear factor $\kappa$B are involved (Huang and Reichardt, 2003). In contrast, substantial evidence indicates that Akt activates a number of effectors involved in protein synthesis (Whiteman et al., 2002; Harris and Lawrence, 2003). A major effector of Akt is mTOR, a kinase that triggers initiation of translation. Overexpression of a membrane targeted Akt in mammalian cells increase mTOR kinase activity as well as mTOR autophosphorylation (Scott et al., 1998; Sekulic et al., 2000). Another effector of Akt is glycogen synthase kinase-3$\beta$ (GSK-3$\beta$). Akt-mediated phosphorylation and inactivation of GSK-3$\beta$ increases the exchange activity of the guanine nucleotide exchange factor eIF-2B and promotes the recruitment of initiator tRNA to the 40S ribosome. Together, it is conceivable that Akt acts as a signaling molecule that links upstream NT-3 signals to the key effectors that control protein synthesis necessary for long-term physiological and morphological changes at the NMJ.

### Role of receptor endocytosis

Endocytosis has long been considered as a mechanism to inactivate receptor-signaling process, but recent studies suggest that, unlike other tyrosine kinase receptors, the endocytosis of neurotrophin-Trk complexes is necessary for several biological effects mediated by neurotrophins (Lu, 2004; Nagappan and Lu, 2005). For example, TrkA endocytosis is required to initiate cell body responses to target-derived NGF; blockade of TrkA internalization by dominant-negative Dynamin prevents NGF-induced neurite outgrowth in PC12 cells (Bhattacharyya et al., 1997; Riccio et al., 1997; Zhang et al., 2000). In the present study, we demonstrate that endocytosis of NT-3-receptor complex represents one of the key mechanisms that separate the acute and long-term synaptic effects of NT-3.

Then, why is endocytosis necessary for long-term, but not acute, effects of NT-3? Or more generally, are there fundamental differences between cell surface and endocytosed receptors in terms of their signaling and functions? It has been shown that epidermal growth factor induces proliferation through a transient activation of MAP kinase, whereas NGF induces differentiation via a sustained activation of the same signaling pathway (Marshall, 1995). NT-3 may activate transient signaling when interacting with cell surface TrkC but more sustained signaling when endocytosed together with its receptor TrkC. Another possibility is that cell surface and endocytosed TrkC receptors activate totally different signaling pathways. NGF activates Ras through cell surface TrkA, leading to a transient activation of MAP kinase, but Rap1 through endocytosed TrkA, resulting sustained MAP kinase (York et al., 2000). Inhibition of receptor endocytosis attenuates MAP kinase activation but increases PI3K signaling (Zhang et al., 2000). Consistent with this, binding of surface TrkA by NGF-beads activates PI3K normally but not MAP kinase (MacInnis and Campenot, 2002). In PC12 cells, the activated NGF-Trk complex is endocytosed into coated vesicles called signaling endosomes (Howe et al., 2001). The extracellular domain of the receptor, now inside the lumen of the vesicles, remains bound to NGF, whereas the intracellular domain of Trk is kept in the phosphorylated state and is catalytically active. This allows its association with signal-generating proteins such as Shc,

Rap1, PLC-γ, etc. (Howe et al., 2001). In addition to the differences in kinetics and downstream signaling molecules, endocytosis takes the receptor to different intracellular locations and makes it less exposed to surface membrane-associated phosphatases. All together, these mechanisms could contribute to the differential signaling between cell surface and endocytosed receptors. It is also conceivable that internalized NT-3-TrkC complexes may be able to differentially activate downstream signaling pathways by using intracellular endosomes, thereby separating the acute and long-term effects of the same neurotrophin.

Our data strongly suggest that a key difference between acute and long-term effects of NT-3 on synaptic modulation is the dependence on NT-3-TrkC endocytosis. However, it should be noted that the concentration of NT-3 used to examine the long-term effect of NT-3 was 20 times lower than that used for the acute effect. We used such a low dose of NT-3 to selectively induce signaling pathways for the long-term effect and therefore distinguish it from the acute effect. As such, however, we cannot completely rule out the possibility that differential dependence on endocytosis may reflect dose rather than time of NT-3 exposure.

## Conclusion

Here, we showed distinct mechanisms that separate two temporarily different actions of neurotrophins by using simple and unique system. These mechanistic differences could be applicable to the neurotrophic regulation of CNS synapses (Lu, 2004). For example, recent studies indicate that long-term neurotrophic treatment of mammalian hippocampal neurons induce dendritic morphological changes (Tyler and Pozzo-Miller, 2001; Ji et al., 2005). Furthermore, several recent studies have demonstrated that BDNF induces PI3K/mTOR-dependent protein synthesis in dendrites of CNS neurons (Schratt et al., 2004; Takei et al., 2004). Some findings such as the requirement for endocytosis of receptors in neurotrophin-mediated long-term synaptic modulation are not established in activity-dependent long-term plasticity. Therefore, it will be interesting to investigate whether similar mechanism is operative in long-term activity-dependent synaptic modulation. In conclusion, these findings, if generalized to other neurotrophic factors, should have a significant impact not only in the understanding of how neurotrophic factors work in the brain but also in the therapeutic application of neurotrophins as drugs for various neurological disorders.

## References


Alessi DR, Cuenda A, Cohen P, Dudley DT, Saltiel AR (1995) PD 098059 is a specific inhibitor of the activation of mitogen-activated protein kinase kinase in vitro and in vivo. J Biol Chem 270:27489–27494.

Baranes D, Lopez-Garcia JC, Chen M, Bailey CH, Kandel ER (1996) Reconstitution of the hippocampal mossy fiber and associational-commissural pathways in a novel dissociated cell culture system. Proc Natl Acad Sci USA 93:4706–4711.

Betz W, Mao F, Bewick G (1992) Activity-dependent fluorescent staining and destaining of living vertebrate motor nerve terminals. J Neurosci 12:363–375.

Bhattacharyya A, Watson FL, Bradlee TA, Pomeroy SL, Stiles CD, Segal RA (1997) Trk receptors function as rapid retrograde signal carriers in the adult nervous system. J Neurosci 17:7007–7016.

Chang S, Popov SV (1999) Long-range signaling within growing neurites mediated by neurotrophin-3. Proc Natl Acad Sci USA 96:4095–4100.

Dai Z, Peng HB (1996) Dynamics of synaptic vesicles in cultured spinal cord neurons in relationship to synaptogenesis. Mol Cell Neurosci 7:443–452.

Davis GW, DiAntonio A, Petersen SA, Goodman CS (1998) Postsynaptic PKA controls quantal size and reveals a retrograde signal that regulates presynaptic transmitter release in *Drosophila*. Neuron 20:305–315.

Evers J, Laser M, Sun Y-A, Xie Z-P, Poo M-M (1989) Studies of nerve-muscle interaction in *Xenopus* cell culture: analysis of early synaptic currents. J Neurosci 9:1523–1539.

Eves EM, Xiong W, Bellacosa A, Kennedy SG, Tsichlis PN, Rosner MR, Hay N (1998) Akt, a target of phosphatidylinositol 3-kinase, inhibits apoptosis in a differentiating neuronal cell line. Mol Cell Biol 18:2143–2152.

Figurov A, Pozzo-Miller LD, Olafsson P, Wang T, Lu B (1996) Regulation of synaptic responses to high-frequency stimulation and LTP by neurotrophins in the hippocampus. Nature 381:706–709.

Gafni J, Munsch JA, Lam TH, Catlin MC, Costa LG, Molinski TF, Pessah IN (1997) Xestospongins: potent membrane permeable blockers of the inositol 1,4,5-trisphosphate receptor. Neuron 19:723–733.

Grimes ML, Zhou J, Beattie EC, Yuen EC, Hall DE, Valletta JS, Topp KS, LaVail JH, Bunnett NW, Mobley WC (1996) Endocytosis of activated TrkA: evidence that nerve growth factor induces formation of signaling endosomes. J Neurosci 16:7950–7964.

Harris TE, Lawrence Jr JC (2003) TOR signaling. Sci STKE 2003:re15.

Howe CL, Valletta JS, Rusnak AS, Mobley WC (2001) NGF signaling from clathrin-coated vesicles. Evidence that signaling endosomes serve as a platform for the Ras-MAPK pathway. Neuron 32:801–814.

Huang EJ, Reichardt LF (2003) Trk receptors: roles in neuronal signal transduction. Annu Rev Biochem 72:609–642.

Ji Y, Pang PT, Feng L, Lu B (2005) Cyclic AMP controls BDNF-induced TrkB phosphorylation and dendritic spine formation in mature hippocampal neurons. Nat Neurosci 8:164–172.

Kaplan DR, Miller FD (2000) Neurotrophin signal transduction in the nervous system. Curr Opin Neurobiol 10:381–391.

Li X, Zhao X, Fang Y, Jiang X, Duong T, Fan C, Huang CC, Kain SR (1998) Generation of destabilized green fluorescent protein as a transcription reporter. J Biol Chem 273:34970–34975.

Lohof AM, Ip NY, Poo MM (1993) Potentiation of developing neuromuscular synapses by the neurotrophins NT-3 and BDNF. Nature 363:350–353.

Lu B (2003) BDNF and activity-dependent synaptic modulation. Learn Mem 10:86–98.

Lu B (2004) Acute and long-term regulation of synapses by neurotrophins. Prog Brain Res 146:137–150.

MacInnis BL, Campenot RB (2002) Retrograde support of neuronal survival without retrograde transport of nerve growth factor. Science 295:1536–1539.

Marshall CJ (1995) Specificity of receptor tyrosine kinase signaling: transient versus sustained extracellular signal-regulated kinase activation. Cell 80:179–185.

Martin K, Casadio A, Zhu H, Yaping E, Rose JC, Chen M, Bailey CH, Kandel ER (1997) Synapse-specific long-term facilitation of *Aplysia* sensory to motor synapses: a function of local protein synthesis in memory storage. Cell 91:927–938.

Mateus C, Avery SV (2000) Destabilized green fluorescent protein for monitoring dynamic changes in yeast gene expression with flow cytometry. Yeast 16:1313–1323.

McAllister AK, Lo DC, Katz LC (1995) Neurotrophins regulate dendritic growth in developing visual cortex. Neuron 15:791–803.

McAllister AK, Katz LC, Lo DC (1999) Neurotrophins and synaptic plasticity. Annu Rev Neurosci 22:295–318.

Nagappan G, Lu B (2005) Activity-dependent modulation of the BDNF receptor TrkB: mechanisms and implications. Trends Neurosci 28:464–471.

Poo MM (2001) Neurotrophins as synaptic modulators. Nat Rev Neurosci 2:24–32.

Powis G, Bonjouklian R, Berggren MM, Gallegos A, Abraham R, Ashendel C, Zalkow L, Matter WF, Dodge J, Grindey G (1994) Wortmannin, a potent and selective inhibitor of phosphatidylinositol-3-kinase. Cancer Res 54:2419–2423.

Raught B, Gingras AC, Sonenberg N (2001) The target of rapamycin (TOR) proteins. Proc Natl Acad Sci USA 98:7037–7044.

Riccio A, Pierchala BA, Ciarallo CL, Ginty DD (1997) An NGF-TrkA-mediated retrograde signal to transcription factor CREB in sympathetic neurons. Science 277:1097–1100.

Ryan TA, Reuter H, Wendland B, Schweizer FE, Tsien RW, Smith SJ (1993) The kinetics of synaptic vesicle recycling measured at single presynaptic boutons. Neuron 11:713–724.

Ryan TA, Ziv NE, Smith SJ (1996) Potentiation of evoked vesicle turnover at individually resolved synaptic boutons. Neuron 17:125–134.

Schratt GM, Nigh EA, Chen WG, Hu L, Greenberg ME (2004) BDNF regulates the translation of a select group of mRNAs by a mammalian target of rapamycin-phosphatidylinositol 3-kinase-dependent pathway during neuronal development. J Neurosci 24:7366–7377.

Scott PH, Brunn GJ, Kohn AD, Roth RA, Lawrence Jr JC (1998) Evidence of insulin-stimulated phosphorylation and activation of the mammalian target of rapamycin mediated by a protein kinase B signaling pathway. Proc Natl Acad Sci USA 95:7772–7777.

Sekulic A, Hudson CC, Homme JL, Yin P, Otterness DM, Karnitz LM, Abraham RT (2000) A direct linkage between the phosphoinositide 3-kinase-AKT signaling pathway and the mammalian target of rapamycin in mitogen-stimulated and transformed cells. Cancer Res 60:3504–3513.

Sun YA, Poo MM (1987) Evoked release of acetylcholine from the growing embryonic neuron. Proc Natl Acad Sci USA 84:2540–2544.

Takei N, Inamura N, Kawamura M, Namba H, Hara K, Yonezawa K, Nawa H (2004) Brain-derived neurotrophic factor induces mammalian target of rapamycin-dependent local activation of translation machinery and protein synthesis in neuronal dendrites. J Neurosci 24:9760–9769.

Tyler WJ, Pozzo-Miller LD (2001) BDNF enhances quantal neurotransmitter release and increases the number of docked vesicles at the active zones of hippocampal excitatory synapses. J Neurosci 21:4249–4258.

Vlahos CJ, Matter WF, Hui KY, Brown RF (1994) A specific inhibitor of phosphatidylinositol 3-kinase, 2-(4-morpholinyl)-8-phenyl-4H-1-benzopyran-4-one (LY294002). J Biol Chem 269:5241–5248.

Wang CY, Yang F, He XP, Je HS, Zhou JZ, Eckermann K, Kawamura D, Feng L, Shen L, Lu B (2002) Regulation of neuromuscular synapse development by glial cell line-derived neurotrophic factor and neurturin. J Biol Chem 277:10614–10625.

Wang T, Xie KW, Lu B (1995) Neurotrophins promote maturation of developing neuromuscular synapses. J Neurosci 15:4796–4805.

Wang X, Berninger B, Poo M (1998) Localized synaptic actions of neurotrophin-4. J Neurosci 18:4985–4992.

Wang XH, Poo MM (1997) Potentiation of developing synapses by postsynaptic release of neurotrophin-4. Neuron 19:825–835.

Watson FL, Heerssen HM, Moheban DB, Lin MZ, Sauvageot CM, Bhattacharyya A, Pomeroy SL, Segal RA (1999) Rapid nuclear responses to target-derived neurotrophins require retrograde transport of ligand-receptor complex. J Neurosci 19:7889–7900.

Watson FL, Heerssen HM, Bhattacharyya A, Klesse L, Lin MZ, Segal RA, Moheban DB, Sauvageot CM, Pomeroy SL (2001) Neurotrophins use the Erk5 pathway to mediate a retrograde survival response. Nat Neurosci 4:981–988.

Whiteman EL, Cho H, Birnbaum MJ (2002) Role of Akt/protein kinase B in metabolism. Trends Endocrinol Metab 13:444–451.

Yang F, He X, Feng L, Mizuno K, Liu X, Russell J, Xiong W, Lu B (2001) PI3 kinase and IP3 are both necessary and sufficient to mediate NT3-induced synaptic potentiation. Nat Neurosci 4:19–28.

York RD, Molliver DC, Grewal SS, Stenberg PE, McCleskey EW, Stork PJ (2000) Role of phosphoinositide 3-kinase and endocytosis in nerve growth factor-induced extracellular signal-regulated kinase activation via Ras and Rap1. Mol Cell Biol 20:8069–8083.

Zhang X, Poo MM (2002) Localized synaptic potentiation by BDNF requires local protein synthesis in the developing axon. Neuron 36:675–688.

Zhang Y, Moheban DB, Conway BR, Bhattacharyya A, Segal RA (2000) Cell surface Trk receptors mediate NGF-induced survival while internalized receptors regulate NGF-induced differentiation. J Neurosci 20:5671–5678.

Zhao H, Nonet ML (2000) A retrograde signal is involved in activity-dependent remodeling at a *C. elegans* neuromuscular junction. Development 127:1253–1266.

Zhu Y, Yang GY, Ahlemeyer B, Pang L, Che XM, Culmsee C, Klumpp S, Krieglstein J (2002) Transforming growth factor-beta 1 increases bad phosphorylation and protects neurons against damage. J Neurosci 22:3898–3909.